Lateglacial to Holocene relative sea-level changes in the Stykkishólmur area, northern Snæfellsnes, Iceland

JQS

MARTIN D. BRADER,[1]* JEREMY M. LLOYD,[1] MICHAEL J. BENTLEY[1] and ANTHONY J. NEWTON[2]
[1]Department of Geography, University of Durham, Durham, UK
[2]School of GeoSciences, Institute of Geography and the Lived Environment, University of Edinburgh, UK

ABSTRACT: Comparatively little research has been undertaken on relative sea-level (RSL) change in western Iceland. This paper presents the results of diatom, tephrochronological and radiocarbon analyses on six isolation basins and two coastal lowland sediment cores from the Stykkishólmur area, northern Snæfellsnes, western Iceland. The analyses provide a reconstruction of Lateglacial to mid-Holocene RSL changes in the region. The marine limit is measured to 65–69 m above sea level (asl), with formation being estimated at 13.5 cal ka BP. RSL fall initially occurred rapidly following marine limit formation, until ca. 12.6 cal ka BP, when the rate of RSL fall decreased. RSL fell below present in the Stykkishólmur area during the early Holocene (by ca. 10 cal ka BP). The rates of RSL change noted in the Stykkishólmur area demonstrate lesser ice thicknesses in Snæfellsnes than Vestfirðir during the Younger Dryas, when viewed in the regional context. Consequently, the data provide an insight into patterns of glacio-isostatic adjustment surrounding Breiðafjörður, a hypothesized major ice stream at the Last Glacial Maximum. © 2015 The Authors. Journal of Quaternary Science published by John Wiley & Sons, Ltd.

KEYWORDS: diatom; Iceland; isolation basin; reconstruction; sea level.

Introduction

During the Last Glacial Maximum (LGM), Iceland was covered by a considerable ice mass (Ingólfsson *et al.*, 2010). However, in comparison with the UK and Fennoscandia, the extent and configuration of the LGM Icelandic Ice Sheet (IIS) is still relatively poorly understood, particularly in the northwest (Andrews and Helgadóttir, 2003). Determining the scale of the LGM IIS is important, as freshwater input to the North Atlantic during deglaciation could have affected global thermohaline circulation (Hubbard *et al.*, 2006). Consequently, various techniques have been used to reconstruct the LGM IIS, including submerged feature mapping (e.g. Ólafsdóttir, 1975; Spagnolo and Clark, 2009), glacial striation identification (e.g. Keith and Jones, 1935; Hoppe, 1982), sedimentology (e.g. Andrews *et al.*, 2000), ice sheet modelling (Hubbard *et al.*, 2006) and ice stream investigation (e.g. Bourgeois *et al.*, 2000). In addition, relative sea-level (RSL) studies have been used to determine the patterns of deglaciation in Iceland, through both marine limit and geomorphological mapping (e.g. Ingólfsson, 1991; Norðdahl and Pétursson, 2005) and isolation basin study (e.g. Rundgren *et al.*, 1997). Despite this range of approaches, there remains uncertainty surrounding the vertical and lateral extent of the LGM IIS (Rundgren and Ingólfsson, 1999) and the associated style and pattern of deglaciation (Norðdahl *et al.*, 2008).

One important area for LGM IIS investigations is Breiðafjörður, a large fjord separating Vestfirðir and Snæfellsnes (Fig. 1), as it was potentially the location of a major ice stream (Bourgeois *et al.*, 2000; Hubbard *et al.*, 2006). Previous research has investigated several features within the region, highlighting the potential maximum ice sheet extent at the LGM (e.g. Ólafsdóttir, 1975), former ice flow dynamics (Bourgeois *et al.*, 2000) and marine limit elevations (e.g. Norðdahl and Pétursson, 2005; Fig. 1). The study of RSL on the northern coastline of Breiðafjörður has also provided an accurate age for deglaciation, alongside the

rates of associated glacio-isostatic adjustment (GIA) over the Lateglacial and Holocene (Lloyd *et al.*, 2009; Fig. 1).

In this paper, we present the results of RSL study from Snæfellsnes, on the southern coast of Breiðafjörður, with the aim of reconstructing postglacial RSL change to investigate deglaciation and ice loading patterns, through comparison with existing datasets. Six isolation basins and two coastal lowland cores were investigated, alongside mapping of the local marine limit, to produce a record of postglacial RSL change. This record provides an opportunity to determine rates of GIA for comparison with Bjarkarlundur, situated 60 km north-northeast on the northern coast of Breiðafjörður (Lloyd *et al.*, 2009).

Previous Research

Because of limited empirical evidence of LGM IIS extent, ice-sheet modelling studies have relied on a small number of dated raised shoreline and marine limit sites and a suite of undated marine limit elevations (e.g. Le Breton *et al.*, 2010). The marine limit elevation, or highest point reached by postglacial sea level (Andrews, 1970), is linked to the timing of deglaciation at particular locations. It is therefore important to establish the age of marine limit formation, providing an opportunity to predict ice thickness and extent, when integrated into GIA models. Unfortunately, marine limit and raised shoreline sites often suffer from a lack of dateable material (e.g. Principato, 2008) and poor spatial coverage, as well as having difficulties in relating the feature formation to mean sea level (Lloyd *et al.*, 2009). Despite this, several existing RSL and deglacial records have been developed using geomorphological evidence (Norðdahl and Pétursson, 2005; Norðdahl *et al.*, 2008).

Previous research has highlighted the spatial variability of marine limit and raised shoreline elevations in western Iceland (e.g. Hjort *et al.*, 1985; Hansom and Briggs, 1991; Ingólfsson, 1991; Norðdahl and Ásbjörnsdóttir, 1995; Norðdahl and Pétursson, 2005). The postglacial marine limit in Breiðafjörður ranges from 80 m asl in Bjarkarlundur (Lloyd *et al.*, 2009) to 110 m asl in inner Breiðafjörður (Norðdahl and Pétursson, 2005; Fig. 1). A small number of these locations have been dated (e.g. Norðdahl and Pétursson,
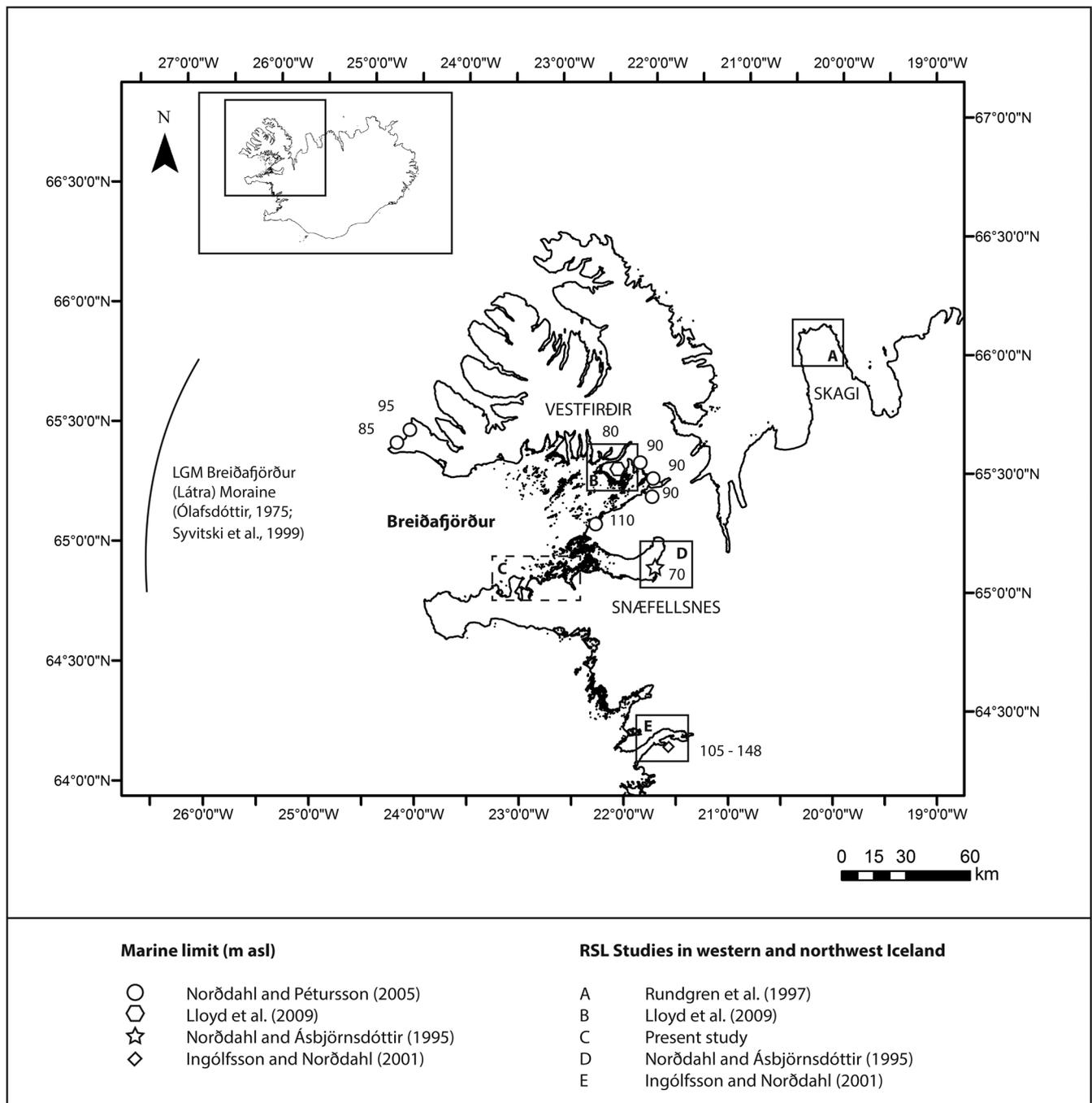
Figure 1. Map of north-west Iceland showing the marine limit elevation, submerged glacial features and relative sea-level studies within Breiðafjörður. The study site is area C.

2005). In addition to the studies of highest postglacial RSL, previous research has also highlighted a period of low RSL at ca. 10.2–10.6k cal a BP in western Iceland (Thors and Helgadóttir, 1991; Ingólfsson et al., 1995; Norðdahl and Pétursson, 2005). Submerged peats at −17 to −30 m asl have demonstrated a minimum position of postglacial RSL in western Iceland (Thors and Helgadóttir, 1991; Ingólfsson et al., 1995) and submerged terraces have demonstrated low points of −40 m asl (Norðdahl and Pétursson, 2005).

Isolation basin sediments have been widely used to construct comprehensive postglacial RSL records for several locations, including Norway (Kjemperud, 1986), Russia (Corner et al., 2001), the UK (Shennan et al., 2000) and Greenland (Long et al., 1999). Isolation basin studies have also been previously undertaken in Iceland (e.g. Rundgren et al., 1997; Lloyd et al., 2009). These RSL records can act as

important tests for models of GIA, providing an opportunity to investigate rates of isostatic uplift or subsidence over time. The first isolation basin study in Iceland was undertaken in northernmost Skagi (Fig. 1), demonstrating a total fall in RSL of 45 m at an average rate of −15.5 mm cal a^{-1} between ca. 13.2 and ca. 10.3k cal a BP, during which two transgressions of 5-m amplitude occurred (Rundgren et al., 1997). These transgressions have been linked to expansions of the IIS during the Younger Dryas and Preboreal (Rundgren et al., 1997; Norðdahl and Pétursson, 2005).

In Bjarkarlundur, Vestfirðir, a fall in RSL of ~80 m since deglaciation has been demonstrated (Lloyd et al., 2009). The research highlights two periods of rapid RSL change, with a rate of −38 mm cal a^{-1} during the Bølling–Allerød and −16 mm cal a^{-1} during the early Holocene (Lloyd et al., 2009). It was noted that the Younger Dryas reduced the rate

of RSL fall in southern Vestfirðir to −4 mm cal a⁻¹ (Lloyd et al., 2009). In Bjarkarlundur, RSL fell below present around 9 cal ka BP, which correlates with the isolation basin record from Skagi (Rundgren et al., 1997) alongside records generated by other sources (Norðdahl and Pétursson, 2005). This fall below present at Bjarkalundur was followed by a transgression during the late Holocene from which RSL is assumed to have fallen to present (Lloyd et al., 2009).

Furthermore, RSL study in western Iceland has demonstrated a series of raised shoreline features from the marine limit to close to present sea level (Ingólfsson, 1988; Ingólfsson and Norðdahl, 2001; Norðdahl and Pétursson, 2005; Norðdahl et al., 2008; Ingólfsson et al., 2010). Ingólfsson and Norðdahl (2001) report marine limit shorelines at 105 and 148 m asl in Akrafjall and Stóri-Sandhóll, Borgarfjörður, western Iceland, with Stóri-Sandhóll dating to ca. 15.45 ± 0.245k cal a BP (uncorrected). A second extensive Younger Dryas shoreline is reported at 60–70 m asl (Ingólfsson and Norðdahl, 2001). The high marine limit elevations in the Borgarfjörður region are taken to be a consequence of rapid deglaciation in western Iceland (Ingólfsson and Norðdahl, 2001).

Research location

Snæfellsnes is a large peninsula in western Iceland, forming the southern coastline of Breiðafjörður (Figs 1 and 2). Snæfellsnes is dominated by the ice-capped Snæfellsjökull volcanic system, which is situated to the extreme west of the peninsula. The geology of the area is characterized by the Snæfellsnes Volcanic Belt which overlies Tertiary basalts and trends from east to west, contrasting with the typical north–south trend of the central volcanic zones (Sigurdsson, 1970). The region is classified as tectonically inactive, despite several small magnitude seismic events between 1912 and 1962 (Sigurdsson, 1970).

Methodology

This research uses a combination of bio- and lithostratigraphic data to investigate RSL changes using a range of field and laboratory methods. The key technique employed in this research is the isolation basin methodology (Kjemperud, 1986). Isolation basins are rock depressions, which have over time been inundated by and isolated from marine conditions (Lloyd et al., 2009), denoted by an isolation contact within the sediments. Kjemperud (1986) notes three isolation contacts within isolation basins: sedimentological, hydrological and diatomological. An accurate record of environmental change is preserved due to the impervious rock 'sill' (Lloyd and Evans, 2002), the altitude of which must be accurately measured, as it is the point which controls the dominant environmental conditions (marine, brackish or freshwater) at each site.

Potential isolation basin sites for analysis were identified in the field using the characteristics outlined by Long et al. (2011). Initial site stratigraphies were determined by coring transects using a gouge corer, with samples for analysis retrieved using a Russian or Livingstone corer depending on the site stratigraphy. Sediments were extracted from an infilled section of the basin or from the rear of a small boat where the lake covered most of the basin. Sediments were described using the Troëls-Smith (1955) classification scheme.

Samples were prepared for diatom analysis using the standard techniques outlined by Palmer and Abbott (1986). A minimum of 250 diatoms were enumerated per sample, using a range of taxonomic guides for identification (e.g. Brun, 1965; Foged, 1972 1973, 1977; Hartley, 1996). Following identification, diatoms were grouped into five classes: marine, brackish, salt tolerant, freshwater and salt intolerant (Hustedt, 1957). Within this paper, summary diagrams are provided for each site, with full diatom counts available as supplementary information (Table S1).

To determine the elevation of former RSL, the indicative meaning should be subtracted from the sill altitude (see Shennan et al., 1999). The indicative meaning is defined as the relationship between the dated sea-level index point and the tidal frame (Van Der Plassche, 1986), which was determined by combined bio- and lithostratigraphic analysis at each location to identify the hydro- and diatomological isolation contacts (Kjemperud, 1986). Mean high water spring tide (MHWST) is frequently used for the diatomological isolation contact (Lloyd et al., 2009; Long et al., 2011), which is characterized by predominantly freshwater conditions with a minor brackish element (Shennan et al., 1994). The hydrological isolation contact represents entirely freshwater conditions and equates to highest astronomical tide (HAT; Shennan et al., 1994).

Tephrochronology and radiocarbon dating were used to provide chronological control for the diatomological isolation contacts. The major element composition of tephra layers was determined by wavelength dispersive analyses on a five-spectrometer Cameca SX100 electron microprobe at the Tephra Analytical Unit, University of Edinburgh. Tephra samples were subjected to an acid digestion before analysis (Persson, 1971) and were subsequently sieved at 63 and 125 μm (e.g. Larsen et al., 1999). Tephra results were compared with previously published compositions using Tephrabase to identify individual horizons (Newton, 1996; Newton et al., 2007). Radiocarbon samples were generated as accelerator mass spectrometry bulk dates from organic sediments close to the diatomological isolation contact, following standard preparation techniques. Radiocarbon ages were subsequently calibrated using CALIB 7.0 (Stuiver et al., 2005) and the IntCal13 calibration dataset (Reimer et al., 2013).

Results

Sites were selected at a range of altitudes from present sea level to the marine limit to investigate RSL changes throughout the Lateglacial and Holocene. Samples were collected from a small geographical area to minimize the impacts of differential rates of isostatic rebound (Fig. 2). Radiocarbon analyses at each site are summarized in Table 1 as 2σ ranges, with tephra geochemistries presented in Table S2.

Borgarland 10 (65°2′40.78N, 22°43′35.51W) core elevation: +1.7 m asl

Borgarland is an extensive coastal lowland area grading into a modern salt marsh to the north of Helgafell on the Thorsnes peninsula (Fig. 2). The lowland contains a former natural channel and later man-made drainage system. A total of 18 diatom samples were analysed, showing a transition from predominantly brackish to mainly freshwater conditions, with a minor brackish component towards the top of the core (Fig. 3A; Appendix). The diatomological isolation contact at 50 cm yields a radiocarbon age for the decrease in marine influence of 7156–7252 cal a BP.

Borgarland 11 (65°2′40.78N, 22°43′35.51W) core elevation: +3.3 m asl

A second core, Borgarland 11, was taken close to the location of Borgarland 10 (Fig. 2; Appendix). Four diatom samples were counted to a minimum of 250 diatoms, but preservation
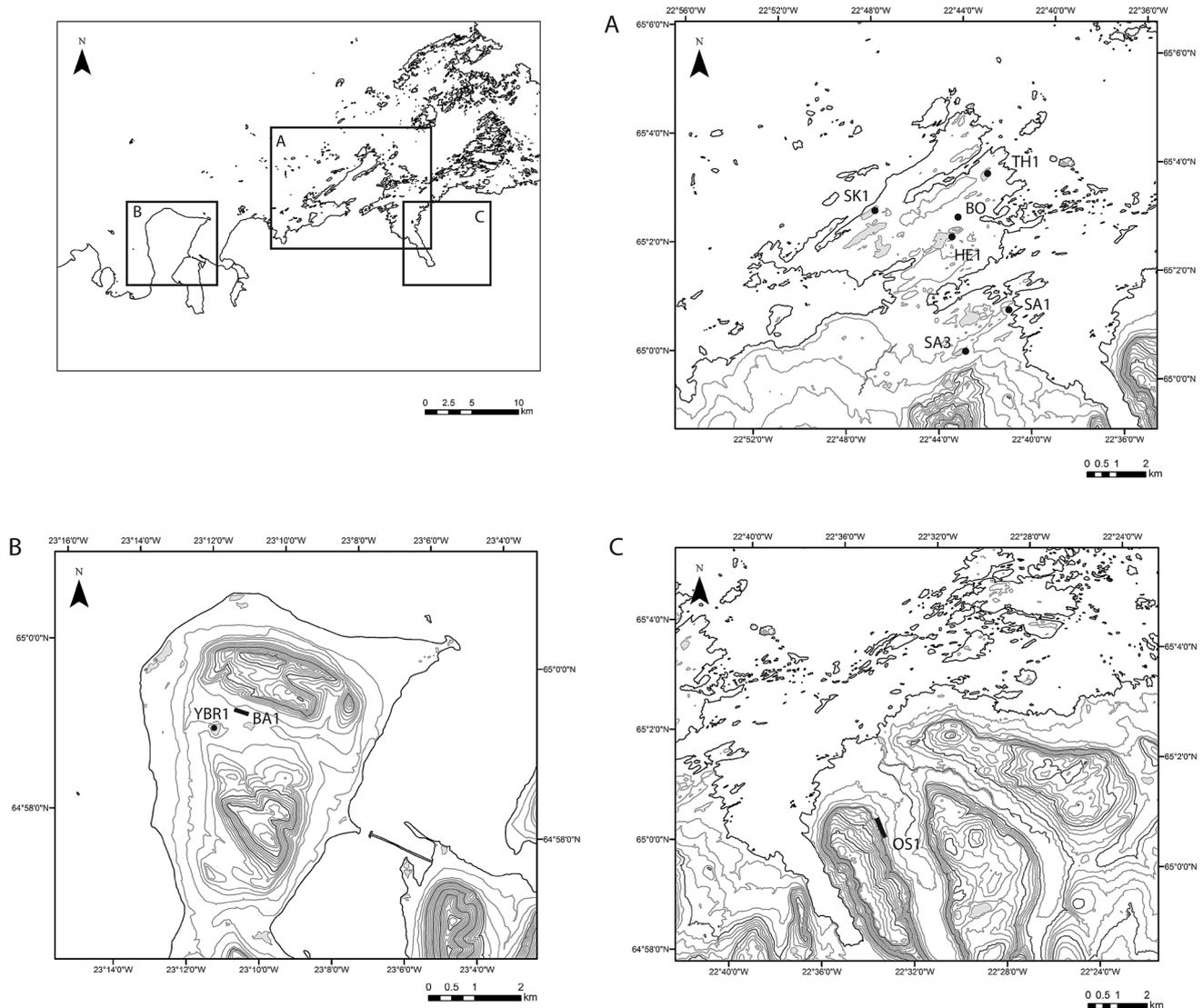
Figure 2. Location of isolation basins (SK1, Skjaldarvatn; TH1, Þingvallavatn; HE1, Helgafellsvatn; SA1, Saurar 1; SA3, Saurar 3; YBR1, Ytra-Bárvatn; circles), coastal lowland (BO10, Borgarland 10; BO11, Borgarland 11; circles) and marine limit sites (OS1, Ós; BR1, Barar; black circles) in northern Snæfellsnes. (Contour interval - light grey: 20 m; dark grey: 100 m) Basemap is based on data from National Land Survey of Iceland.

was generally poor (Fig. 3B). There were no visible tephra deposits within the sediment core. The diatom flora indicate a brackish–marine signal from the base of the core up to 104 cm (Fig. 3B). A radiocarbon date from 104 cm dates the transition from brackish to fully freshwater conditions to 9915–10 097 cal a BP.

Skjaldarvatn (65°2′50.67N, 22°47′11.35W) sill altitude: +4.4 m asl

Skjaldarvatn is located to the south-west of the Thorsnes peninsula (Fig. 2). The basin is elongated, 700 m long and 180 m wide and has an infilled section to the north-east of

Table 1. Chronological analyses and sea-level index points from isolation basins and coastal lowland sites within this study (to 1 decimal place). All samples for radiocarbon analysis have undergone a standard acid wash pretreatment.

| Site	Lab. code	^{14}C age (1σ) (^{14}C a BP)	Calibated age age (2σ) (cal a BP)	Sill/core altitude (m)	Core depth (cm)	Indicative meaning	Mean sea level (m)
Borgarland 10	Poz- 43545	6240 ± 40	7148–7259	1.7	50	MHWST	−0.2
Borgarland 11	SUERC-47976	8931 ± 39	9915–10 097	3.3	104	HAT	0.9
Skjaldarvatn	SUERC-47977	9973 ± 44	11 253–11 619	4.4	548	MHWST	2.6
Þingvallavatn	Poz- 43546	9710 ± 60	11 066–11 241	5.3	505	MHWST-HAT	3.2
Saurar 1	SUERC-47983	10 455 ± 43	12 135–12 544	9.0	332	MHWST-HAT	6.8
Saurar 1	SUERC-47982	10 682 ± 44	12 569–12 713	9.0	336	N/A	N/A
Helgafellsvatn	SUERC-47980	9493 ± 41	10 650–10 834	12.8	575	N/A	N/A
Helgafellsvatn	SUERC-47981	9914 ± 42	11 224–11 408	12.8	620	MHWST-HAT	10.6
Saurar 3	Poz- 43547	10 670 ± 60	12 544–12 722	16.2	808	MHWST-HAT	14.1
Ytra-Bárvatn	SUERC-47984	6972 ± 35	7702–7869	57.6	210	N/A	N/A
Ytra-Bárvatn	SUERC-48878	16 841 ± 76	20 074–20 536	57.6	468	MHWST	56.0
Ytra-Bárvatn	BETA-0314	20 140 ± 60	24 340– 24 075	57.6	440	HAT	55.2
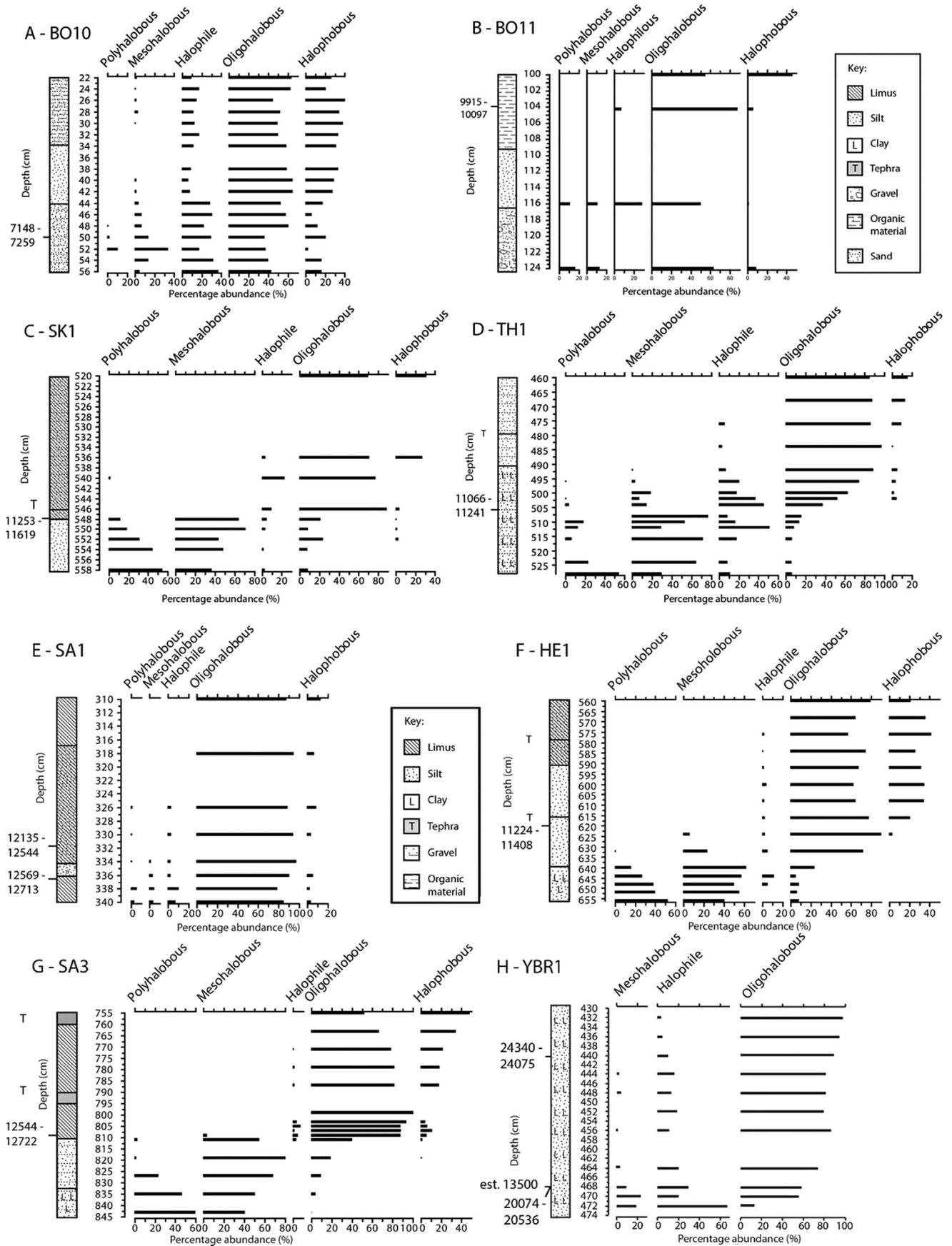
Figure 3. Summary diatom assemblages and lithostratigraphy from isolation basin and coastal lowland sites in Snæfellsnes. Full diatom diagrams are available from the corresponding author upon request. Calibrated ages are reported where appropriate. A, Borgarland 10; B, Borgarland 11; C, Skjaldarvatn; D, Þingvallavatn; E, Saurar 1; F, Helgafellsvatn; G, Saurar 3; H, Ytra-Bárvatn.

Skjaldarvatn lake. Higher ground is found to the north, south and east, with a stream draining the lake to the south-west. The bedrock sill was located within the stream bed, lying at +4.37 m asl. The sample for analysis was retrieved from the infilled section to the north-east (Appendix). A tephra layer at 546 cm was analysed, but could not be geochemically matched to any previously published record. Diatom analysis demonstrates a transition from marine to brackish dominance, followed by freshwater and salt-intolerant species dominance (Fig. 3C). The shift in diatom assemblage from marine–brackish to freshwater dominance at 540 cm represents the isolation contact and is radiocarbon dated to 11 253–11 619 cal a BP (Fig. 3C).

Þingvallavatn (65°3′33.30N, 22°42′43.16W) sill altitude: +5.3 m asl

Þingvallavatn is a basin situated to the north of the Thorsnes peninsula (TH1, Fig. 2). The basin contains a lake approximately 300 m in diameter, with the basin sill being covered by peat, situated to the north-east. A grid of cores led to the sill being identified at +5.34 m asl. Two transects were cored using a boat, with a sample for analysis being collected near the centre of the lake (Appendix). The tephra layers at 456 and 479 cm were analysed, providing chemical signatures that could not be matched to published data. Diatom analyses (Fig. 3D) revealed a basal marine–brackish zone, moving to a transitional brackish phase at 505–498 cm which is then replaced by freshwater conditions. The diatomological isolation contact is at 507 cm, providing a date for isolation of 11 089–11 219 cal a BP.

Saurar 1 (65°1′4.53N, 22°41′47.11W) sill altitude: +9.0 m asl

The Saurar 1 basin is approximately 7 km south of Stykkishólmur (SA1, Fig. 2). Saurar 1 is situated within an area of low, undulating topography and is dissected by a forest road. The basin measures approximately 350 m long by 120 m wide, with an outlet stream draining the site to the north-west. The basin sill was identified based on a grid of cores and a sample was retrieved from the centre of the site (Appendix). Tephra analysis was undertaken on one sample from 334 cm, which demonstrated a mixed geochemical signature. Diatom analysis identified a predominantly freshwater flora throughout the core, but with a significant marine–brackish component to the flora towards the base of the core. The diatomological isolation contact is at 332 cm, which was radiocarbon dated to 12 135–12 544 cal a BP (Fig. 3E).

Helgafellsvatn (65°2′18.87N, 22°44′23.25W) sill altitude: +12.8 m asl

Helgafellsvatn is situated below Helgafell, a small hill of 60 m, which dominates the local landscape (HE1, Fig. 2). The basin consists of a lake approximately 750 m long and 400 m wide, as well as an extensive infilled section to the north-east. The basin sill was located close to the church at Helgafell. A transect of cores were taken from the infilled section at the lake edge, with a sample for analysis being extracted close to the centre of the transect (Appendix). The tephra layers at 578 and 615 cm are geochemically similar in composition but could not be identified and therefore were unable to assist in the constraint of isolation. Diatom analysis shows a lower marine–brackish zone (660–635 cm), an intermediate transitional zone (635–616 cm) and an upper freshwater zone (616–560 cm). The diatomological isolation

contact at 616 cm was radiocarbon dated, providing an age of 11 224–11 408 cal a BP (Fig. 3F).

Saurar 3 (65°0′18.79N, 22°43′6.19W) sill altitude: +16.2 m asl

The basin at Saurar 3 is located along the same forest road as Saurar 1 (Fig. 2). The basin is made up of a large lake and bog, with the basin measuring 570 m by 180 m. Higher ground is found to the north, west and east, with a lower lying area to the south. The basin sill was identified through a coring grid to the south of the lake. A transect of cores was investigated to the north of the lake. A sample for analysis was collected using a Livingstone corer towards the centre of the core transect (Appendix). Geochemical analysis was undertaken on the two tephra layers. The upper tephra layer at 755 cm had a distinct Veiðivötn-type signature, with the lower deposit at 790 cm probably being sourced from Grímsvötn. Diatom analysis identified a transition from a basal marine–brackish zone (845–825 cm), to a brackish zone (825–810 cm) then an upper freshwater zone from 810 cm. A radiocarbon date from the diatomological isolation contact at 808 cm provided a calibrated age of 12 558–12 646 cal a BP (Fig. 3G).

Ytra-Bárvatn (64°59′2.97N, 23°11′39.34W) sill altitude: +57.6 m asl

Ytra-Bárvatn is located on the Setberg peninsula approximately 20 km west of Stykkishólmur, and consists of a large lake with a diameter of approximately 220 m (YBR1, Fig. 2). The lake is drained to the west by a small stream, with the sill being identified within the stream bed. Higher ground is found to the north and south, with the basin situated within a small valley. The basin is situated below the highest raised shoreline identified in the area and thus provides a minimum age for highest postglacial sea level. Two perpendicular transects were cored within the basin to establish site stratigraphy, with a sample being taken from the northern part of the lake, which yielded thicker sediments (Appendix). Within the core sample, two distinct tephra horizons at 210 and 354 cm underwent geochemical analysis. The upper tephra deposit did not have a homogeneous geochemical signature, being of mixed origin. However, the lower tephra deposit demonstrates a correlation with the Saksunarvatn tephra, providing an age of 10 210 ± 35 cal a BP (Lohne et al., 2014; Fig. 4). A radiocarbon date from the diatomological isolation contact at 468 cm returned a calibrated age of 20 074–20 536 cal a BP; Fig. 3H. A second date at 440 cm returned an age of ~24 000 cal a BP, suggesting a problem with contamination by old carbon at the site.

Discussion

Marine limit formation in northern Snæfellsnes

In the Stykkishólmur area, the highest raised shorelines were measured between 65 m (BR1) and 69 m (OS1) asl (Fig. 2). These local marine limit values are lower than postglacial marine limits identified on the northern shore of Breiðafjörður at 78–98 m (Lloyd et al., 2009) and those identified in inner Breiðafjörður at 90–110 m (Norðdahl and Pétursson, 2005). However, the marine limit elevation identified in the Stykkishólmur area is similar to the altitude of the postglacial marine limit from Skagi at 65 m (Rundgren et al., 1997) and elsewhere in western Iceland at 60–70 m (Ingólfsson, 1991), which formed during the Bölling Period (Norðdahl and Pétursson, 2005). In addition, the marine limit lies at a similar
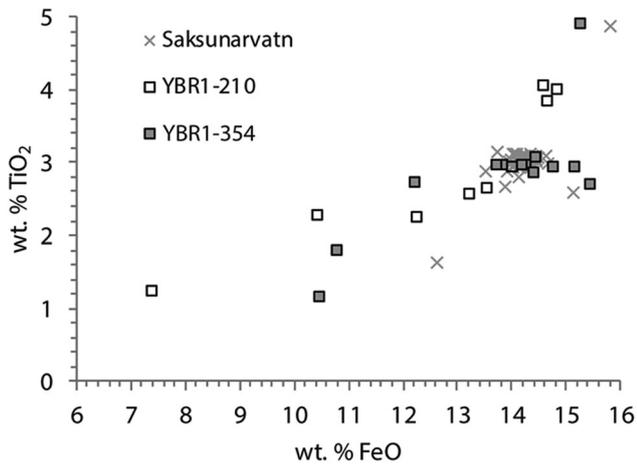
Figure 4. Tephra geochemistry for Ytra-Bárvatn, northern Snæfellsnes. Saksunarvatn data from Tephrabase (www.tephrabase.org; Newton, 1996). Analytical conditions: beam voltage, 15 kV; beam current, 2 nA for Si, K, Al, Fe, Mg, Na and Ca and 80 nA for Ti, Mn and P; beam size, 8 μm. A mixture of minerals, metals and artificial glasses were used to calibrate the instruments and analytical stability was checked using a BCR2G standard.

Figure 5. Age–depth profile for Ytra-Bárvatn, showing the possible ages of isolation at the site.

elevation to the Younger Dryas marine limit identified in innermost Breiðafjörður (Norðdahl and Ásbjörnsdóttir, 1995). Consequently, if the Stykkishólmur area marine limit is to be used to assess GIA in the region, detailed chronological control of the marine limit is needed, as marine limits of similar elevation appear not to have all formed simultaneously.

Isolation basin studies provide an opportunity to determine the age of the marine limit at a given location and also the minimum age for deglaciation where sites with elevations close to the marine limit are available (e.g. Lloyd et al., 2009). Ytra-Bárvatn, the highest basin investigated in this study, at 57.6 ± 0.6 m asl could therefore provide a minimum date for deglaciation in northern Snæfellsnes. The diatom assemblage of Ytra-Bárvatn demonstrates a weak brackish signal towards the base of the core sample (Fig. 3H). This probably indicates a weak marine signal, as the basin is close to isolation and therefore only inundated for part of the tidal cycle.

Three radiocarbon dates were obtained at Ytra-Bárvatn to establish the timing of the decrease in marine influence at the site and establish the age of tephra deposits found in the sediment sample retrieved. The lowest bulk sediment sample at 468 cm provided an age of 16 841 ± 76 ^{14}C a BP (20 074–20 536 cal a BP), which is considerably older than previously reported isolation basin records (e.g. Rundgren et al., 1997; Lloyd et al., 2009). This sample was organic-poor and it is therefore likely that the age generated is misrepresentative of the basin isolation, being affected by the in-washing of carbon from the surrounding landscape (Björck and Wohl-farth, 2001) or reservoir effects. Björck and Wohlfarth (2001) have demonstrated that similar organic-poor sediments have produced dates which are thousands of years older than organic-rich sediments in similar settings. Previous research has highlighted that plant macrofossils provide the most reliable dating constraints from lake sediments (Abbott and Stafford, 1996), but the lack of identifiable plant macrofossils within the isolation basin sediments led to the use of bulk accelerator mass spectrometry dates in this study. Similar limitations have been highlighted in other isolation basin records in Iceland (e.g. Lloyd et al., 2009).

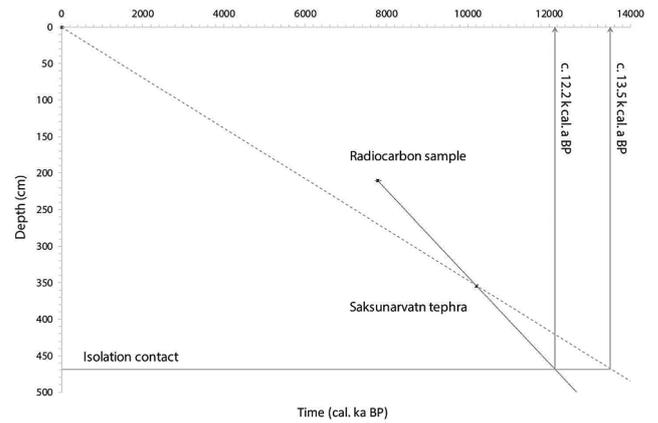Consequently, the date produced from the commencement of organic sedimentation at the site may be more representative of basin isolation, once the position within the tidal frame represented has been established. However, a second date at 440 cm provided an even older age (Table 1), suggesting a problem with old carbon contamination at the site. The upper tephra deposits within the Ytra-Bárvatn sediment sample were of mixed geochemistry and therefore probably represent the reworking of tephra from the surrounding landscape. The geochemical analysis of the lower tephra deposit at YBR1, however, demonstrates a good correlation to the Saksunarvatn tephra (Fig. 4). Using this as a chronological marker (10 210 ± 35 cal a BP, Lohne et al., 2014) and assuming constant sedimentation throughout the core sample, it is possible to estimate the timing of isolation at the site, if all radiocarbon ages are discounted (due to potential contamination). If these two assumptions are accepted, basin isolation can be estimated to ca. 13 500 cal a BP (Fig. 5). Indeed, this is likely to be a minimum age, as the rate of sedimentation is likely to be relatively lower initially after isolation of the basin (relatively organic-poor accumulation), rising slightly as organic content increases.

Extrapolation using the sedimentation rate between the upper radiocarbon date at 210 cm and Saksunarvatn tephra at 354 cm provides a younger age of isolation of ca. 12.2 cal a BP, which would correlate well with the Younger Dryas shorelines in inner Breiðafjörður (Norðdahl and Ásbjörnsdóttir, 1995). The full range of possible ages for isolation of Ytra-Bárvatn are therefore plotted on Fig. 5. However, the younger extrapolated isolation age is younger than isolation ages of lower basins, such as SA1 and SA3. For this scenario to be accepted, both lower basins would need to be affected by contamination from older carbon within the landscape. While this is possible, our preferred interpretation is for an age for the isolation of YBR1 of ca. 13.5 cal ka BP, which correlates well with the results of Lloyd et al. (2009).

Accordingly, we propose that the marine limit identified in the Stykkishólmur area formed before the Younger Dryas, supported by the radiocarbon ages retrieved from lower elevation sites. Previous studies in the Bjarkarlundur area (Lloyd et al., 2009), northernmost Skagi (Rundgren et al., 1997) and lower Borgarfjörður (Ingólfsson and Norðdahl, 2001) have determined ages of 14 125 ± 340, >14 000 and 15 450 ± 245 cal a BP, respectively, for the marine limit shorelines in these areas. The estimated age of the marine limit in the Stykkishólmur area based on the isolation of Ytra-Bárvatn (>13 500 cal a BP), therefore, appears reasonable.
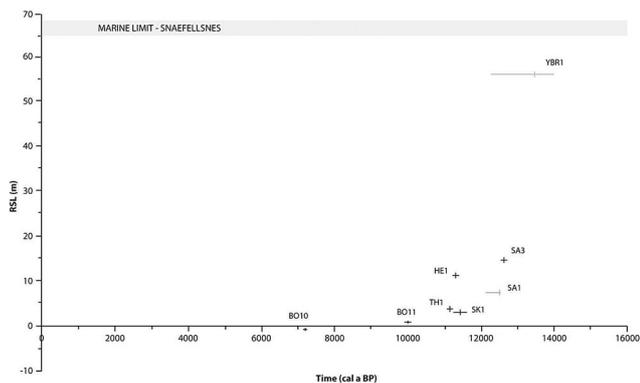
Figure 6. RSL curve for northern Snæfellsnes, with sea-level index points plotted against calibrated ages. Sea-level index point at HE1 is not used to constrain the curve due to a presumed incorrect age of isolation. Black crosses represent sea-level index points, with grey crosses showing limiting ages.

Lateglacial to mid-Holocene RSL change

The six isolation basin and two coastal lowland sites investigated in northern Snæfellsnes constrain the RSL change during the Lateglacial to mid-Holocene (Table 1; Fig. 6). Based on our preferred interpretation a new RSL curve for the Stykkishólmur area has been constructed using the isolation basin and coastal lowland sea-level index points (Fig. 6), with chronological control being provided through radiocarbon dates and tephra analysis.

Following deglaciation, RSL fell rapidly over the course of the Lateglacial and early Holocene in northern Snæfellsnes. Following the isolation of Ytra-Bárvatn (YBR1, 57.6 m asl) RSL fall occurred rapidly until the isolation of Saurar 3 (SA3, 16.2 m asl) at 12 544–12 722 cal a BP (Fig. 6). This RSL fall demonstrates the rapid rate of isostatic rebound, which is comparable to regional trends (Lloyd *et al.*, 2009). This correlation is likely given the relative proximity of the two study areas (~60 km) (Fig. 1). The rates of initial RSL fall and isostatic rebound reported in Skagi (Rundgren *et al.*, 1997) are notably lower than those reported for the Stykkishólmur and Bjarkarlundur areas (Lloyd *et al.*, 2009).

Following the isolation of Saurar 3 (SA3, 16.2 m asl), the rate of RSL change decreased to −24.5 mm cal a^{-1} until the isolation of Saurar 1 (SA1, 9.0 m asl) at 12 135–12 544 cal a BP. This reduced rate of RSL change corresponds to a decrease in the rate of isostatic rebound to +46 mm cal a^{-1}, when eustatic sea-level changes over the period are taken into consideration (Fairbanks, 1989). Previous studies have demonstrated a similar reduction in the rate of RSL change during this period, associated with the expansion of Younger Dryas ice caps and glaciers (Lloyd *et al.*, 2009).

From the RSL record generated in this study, there is only evidence for a limited Younger Dryas ice readvance, as there is little indication of a notable transgression during this period in the Stykkishólmur area. The RSL curve generated for the Stykkishólmur area suggests an exponential decrease in the rate of glacio-isostatic rebound since deglaciation and thus minimal influence from Younger Dryas ice regrowth. It is also evident that RSL was higher on the northern coast of Breiðafjörður during this period (Lloyd *et al.*, 2009) (Fig. 7). This difference in RSL could be attributed to a larger Younger Dryas ice cap in Vestfirðir than on the Snæfellsnes peninsula (Norðdahl and Pétursson, 2005).

Following the isolation of Saurar 1 (9.0 m asl), RSL fell to between 2.6 and 3.2 m asl, with a decrease in marine influence noted at Skjaldarvatn (SK1) between 11 253 and 11
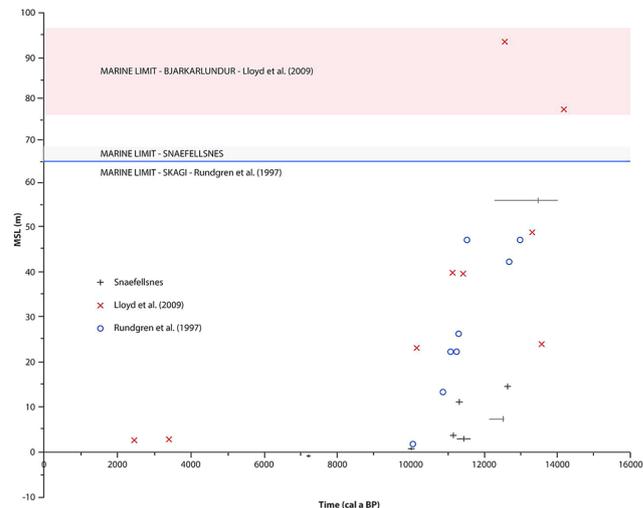

Figure 7. RSL curves from north-west Iceland, demonstrating regional trends and variability between sites investigated in Snæfellsnes (plus (+)), Bjarkarlundur, Vestfirðir (diagonal crosses (x), Lloyd *et al.*, 2009) and Skagi (open circle (o), Rundgren *et al.*, 1997). For Snæfellsnes, black plus symbol (+) represent sea-level index points, with grey showing limiting ages.

619 cal a BP and the isolation of Þingvallavatn (TH1) at 11 066–11 241 cal a BP (Fig. 6). These decreases in marine influence probably occurred in quick succession, as the error associated with the determination of site elevation and decrease in marine influence mean that these events could have occurred concurrently. Both Skjaldarvatn and Þingvalla-vatn have visible tephra deposits close to the point of decreased marine influence.

Þingvallavatn shows a clear shift from marine–brackish to freshwater dominance within the diatom assemblage (Fig. 3D) and contains two tephra layers with geochemical signatures that are unable to be matched to previous records. The geochemical signature attained from analysis of the Skjaldarvatn deposits shows a mixed assemblage, with tephra shards demonstrating Veiðivötn-, Grímsvötn-, Katla- and Snæfellsnes Volcanic Belt-type geochemical compositions (Tephrabase, 2012). It is possible that the geochemical signal highlighted in the Þingvallavatn core is masked at Skjaldar-vatn by the in-washing of additional material from the surrounding landscape. A mixed tephra composition is proba-bly the result of an unvegetated landscape, where tephra can move freely without being trapped by plant material or sediment.

At Skjaldarvatn, the transition between marine–brackish and freshwater dominance is very sharp (Fig. 3C). This transition within the diatom assemblage is probably affected by the tephra deposit at 546 cm, although basin isolation had commenced before this point in the diatom assemblage. As a result, the age of isolation of Skjaldarvatn is older than anticipated due to the radiocarbon age being sought at the point of freshwater dominance rather than the completion of isolation within the diatom assemblage. However, there is relatively little influence on the RSL curve for the region.

It is clear that RSL was between 2.6 and 3.2 m asl between 11 066–11 241 and 11 253–11 619 cal a BP when corrected for the indicative meaning. As a result, the timing of isolation at Helgafellsvatn appears to be anomalous (Figs 5 and 6). The diatom assemblage for the site demonstrates a clear transition between marine–brackish and freshwater dominance, sug-gesting a relatively rapid isolation of the basin (Fig. 3). However, the timing of isolation appears anomalously young compared with the other sites presented here

(11 224–11 408 cal a BP). Based on our preferred interpretation, the date from Helgafellsvatn must therefore be anomalous; hence, it is not used to constrain RSL. An alternative interpretation accepting the age of the isolation contact at Helgafellsvatn would require a rise in RSL of approximately 5 m following the isolation of SA1 at 12 135–12 544 cal a BP, or a larger rise of approximately 8 m following the isolation of SK1 at 11 253–11 619 cal a BP. An additional alternative interpretation is that the isolation contacts for sites SA3, SA1, SK1 and (to a lesser degree) TH1 are too old and the rate of RSL fall during the Lateglacial is rather more gradual than our preferred interpretation suggests.

Mid- to Late Holocene RSL change

Following the isolation of Þingvallavatn (TH1; 5.3 m asl) at 11 066–11 241 cal a BP, a sea-level index point at the coastal marsh site at Borgarland (BO11) records RSL falling below 0.9 m at 9915–10 097 cal a BP (Fig. 6). Following this, RSL probably fell below present; the index point from BO10 records RSL below present (at −0.2 m) by 7148–7259 cal a BP (Fig. 6). This fall below present sea level is later than existing records, which demonstrate a fall below present sea level at ca. 8.2–10.6 ka cal BP (Rundgren *et al.*, 1997; Norðdahl and Pétursson, 2005; Lloyd *et al.*, 2009). The RSL index point from BO10 suggests that RSL probably fell lower than this point during the mid-Holocene. Following this, there are two scenarios: a transgression during the mid-Holocene or a gradual rise to present.

The altitude of transgression during the mid-Holocene is limited by the lack of a second marine incursion recorded in the diatom assemblage from Skjaldarvatn or Þingvallavatn. As a result, RSL did not reach higher than 2.6 ± 0.7 m asl during the mid- to late Holocene in the Stykkishólmur area. There is, however, a short-lived recurrence of mesohalobous species within the Borgarland sequence (BO10, Fig. 3A). Previous studies have noted the potential for Holocene transgressions in Iceland, including in the south-west at 2–6 m asl at 2.9 and 2.3 cal ka BP (Símonarson and Leifsdóttir, 2002) and Hvammsfjörður, western Iceland at 3 and 5 m asl after 4.5 cal ka BP (Norðdahl and Pétursson, 2005; Ingólfsson *et al.*, 2010). To further develop the late Holocene RSL record for Snæfellsnes, additional sites at low elevations are required. However, such sites were not identified in the Stykkishólmur area and sites on the southern coast of the Snæfellsnes peninsula were determined to be unsuitable for isolation basin research due to the nature of the basin sills.

Conclusions

The study of RSL change in the Stykkishólmur area offers an opportunity to investigate GIA on the south coast of Breiðafjörður, when coupled with existing isolation basin and marine limit records from the region. The RSL record from the Stykkishólmur area highlights a difference in patterns of GIA in and around Breiðafjörður since deglaciation. In the Stykkishólmur area, the postglacial marine limit is identified at 63–69 m asl. Previous research has highlighted higher marine limit elevations in northern and innermost Breiðafjörður than determined in this study. This indicates that ice thicknesses were probably greater in northern and innermost Breiðafjörður than in the Stykkishólmur area before deglaciation, or that deglaciation occurred later in the Stykkishólmur area.

RSL fell rapidly following deglaciation on both the northern (Lloyd *et al.*, 2009) and the southern coastlines of Breiðafjörður. The rate of RSL fall in the Stykkishólmur area correlates well with Lloyd *et al.* (2009) when the hypothesized

marine limit age of 13 500 cal a BP is employed. The new RSL record from the Stykkishólmur area also provides an opportunity to explore the consequences of Younger Dryas ice regrowth. There is no evidence for a transgression during the Younger Dryas based on the isolation basin data from the Stykkishólmur area. Instead, the RSL curve shows a decrease in the rate of isostatic rebound from the LGM. There is little evidence for the influence of Younger Dryas ice regrowth in the Stykkishólmur area in the RSL record. This differs from the results on the northern coastline of Breiðafjörður (Lloyd *et al.*, 2009), suggesting variation in ice conditions between the north and south coast of Breiðafjörður during the Younger Dryas, and that the influence of any glacial loading was relatively localized and did not significantly affect the Stykkishólmur area.

During the mid-Holocene, RSL fell below present at 7148–7259 cal a BP following the decrease in marine influence at Borgarland 11 at 9915–10 097 cal a BP. This appears later than noted in previous studies in western Iceland, which have noted an RSL fall below present at ~8.2–10.6 cal ka BP (e.g. Lloyd *et al.*, 2009). There is evidence of a subsequent minor transgression during the Late Holocene reaching less than 2.6 m asl (based on the indicative meaning correction of the sill elevation at Skjaldarvatn). Following this, RSL regressed to present although additional RSL data are required to better constrain these recent RSL changes.

Supplementary information

Additional supporting information can be found in the online version of this article:

Table S1. Full diatom counts from isolation basin and coastal lowland sediment core samples studied in the Stykkishólmur area, northern Snæfellsnes, Iceland.

Table S2. Tephra geochemical data for isolation basin and coastal lowland sites analysed in the Stykkishólmur area, northern Snæfellsnes, Iceland.

Appendix. Lithostratigraphic data from the Stykkishólmur area.

Abbreviations. HAT, highest astronomical tide; IIS, Iceland Ice Sheet; LGM, Last Glacial Maximum; MHWST, mean high water spring tide; RSL, relative sea level.

References

Abbott MB, Stafford TW, Jr. 1996. Radiocarbon geochemistry of modern and ancient Arctic lake systems, Baffin Island, Canada. *Quaternary Research* **45**: 300–311.

Andrews JT. 1970. *A geomorphological study of postglacial uplift: with particular reference to Arctic Canada.* Institute of British Geographers, Special Publication No. 2: London. 156pp.

Andrews JT, Hardardóttir J, Helgadóttir G et al. 2000. The N and W Iceland Shelf: insights into Last Glacial Maximum ice extent and deglaciation based on acoustic stratigraphy and basal radiocarbon AMS dates. *Quaternary Science Reviews* **19**: 619–631.

Andrews JT, Helgadóttir G. 2003. Late Quaternary ice cap extent and deglaciation, Hunafloaáll, northwest Iceland: evidence from marine cores. *Arctic Antarctic and Alpine Research* **35**: 218–232.

Björck S, Wohlfarth B. 2001. 14C chronostratigraphic techniques in paleolimnology. In *Tracking Environmental Change Using Lake Sediments: Physical and Chemical Techniques*, Last WM, Smol JP (guest eds). Kluwer: Dordrecht 205–245.

Bourgeois O, Dauteuil O, Vliet-Lanoë BV. 2000. Geothermal control on flow patterns in the Last Glacial Maximum ice sheet of Iceland. *Earth Surface Processes and Landforms* **25**: 59–76.

Brun J. 1965. *Diatomées des Alpes et du jura*. Asher: Amsterdam. 188 pp.

Corner GD, Kolka VV, Yevzerov VY et al. 2001. Postglacial relative sea-level change and stratigraphy of raised coastal basins on Kola Peninsula, northwest Russia. *Global and Planetary Change* **31**: 155–177.

Fairbanks RG. 1989. A 17,000-year glacio-eustatic sea level record: influence of glacial melting rates on the Younger Dryas event and deep-ocean circulation. *Nature* **342**: 637–642.

Foged N. 1972. The diatoms in four postglacial deposits in Greenland. *Meddelelser om Grønland* **194**: 1–66.

Foged N. 1973. Diatoms from southwest Greenland. *Meddelelser om Grønland* **194**: 1–84.

Foged N. 1977. The diatoms of four postglacial deposits at Godthåbsfjord, west Greenland. *Meddelelser Om Grønland* **199**: 1–64.

Hansom JD, Briggs DJ. 1991. Sea-level changes in Vestfirðir, north west Iceland. In *Environmental Change in Iceland: Past and Present*, Maizels JK, Caseldine C (eds). Kluwer: Dordrecht 79–91.

Hartley B. 1996. *An Atlas of British Diatoms*. Biopress: Bristol. 601pp.

Hjort C, Ingólfsson O, Norðdahl H. 1985. Late Quaternary geology and glacial history of Hornstrandir, northwest Iceland: a reconnaissance study. *Jokull* **35**: 9–29.

Hoppe G. 1982. The extent of the last inland ice sheet in Iceland. *Jökull* **32**: 3–11.

Hubbard A, Sugden D, Dugmore A et al. 2006. A modelling insight into the Icelandic Last Glacial Maximum ice sheet. *Quaternary Science Reviews* **25**: 2283–2296.

Hustedt F. 1957. Diatoméenflora der fluss-systems der Weser im gebeit der Hansestadt Bremen. *Abhandlungen Herausgegeben von Naturwissenschaftlichen Verein zu Bremen* **34**: 181–440.

Ingólfsson Ó. 1988. Glacial history of the lower Borgarfjördur area, western Iceland. *Geologiska Foereningan i Stockholm. Foerhandlingar* **110**: 293–309.

Ingólfsson Ó. 1991. A review of the Late Weichselian and Early Holocene glacial and environmental history of Iceland. In *Environmental Change in Icel and : Past and Present*, Maizels J, Caseldine C (eds). Springer: Amsterdam 13–29.

Ingólfsson Ó, Norðdahl H, Haflidason H. 1995. Rapid isostatic rebound in southwestern Iceland at the end of the last glaciation. *Boreas* **24**: 245–259.

Ingólfsson Ó, Norðdahl H, Schomacker A. 2010. Deglaciation and Holocene glacial history of Iceland. In *The Mýrdalsjökull Ice Cap, Icel and : Glacial Processes, Sediments and Landforms on an active volcano*, Anders Schomacker JK, Kurt HK (eds). Elsevier: Amsterdam 51–68.

Ingólfsson Ó, Norðdahl H. 2001. High relative sea level during the Bolling Interstadial in Western Iceland: a reflection of ice-sheet collapse and extremely rapid glacial unloading. *Arctic Antarctic and Alpine Research* **33**: 231–243.

Keith DB, Jones EW. 1935. Grímsey, North Iceland. *Geographical Journal* **86**: 143–152.

Kjemperud A. 1986. Late Weichselian and Holocene shoreline displacement in the Trondheimsfjord area, central Norway. *Boreas* **15**: 61–82.

Larsen G, Dugmore A, Newton A. 1999. Geochemistry of historical-age silicic tephras in Iceland. *Holocene* **9**: 463–471.

Le Breton E, Dauteuil O, Biessy G. 2010. Post-glacial rebound of Iceland during the Holocene. *Journal of the Geological Society* **167**: 417–432.

Lloyd JM, Evans JR. 2002. Contemporary and fossil foraminifera from isolation basins in northwest Scotland. *Journal of Quaternary Science* **17**: 431–443.

Lloyd JM, Norðdahl H, Bentley MJ et al. 2009. Lateglacial to Holocene relative sea-level changes in the Bjarkarlundur area near Reykholar, North West Iceland. *Journal of Quaternary Science* **24**: 816–831.

Lohne ØS, Mangerud J, Birks HH. 2014. IntCal13 calibrated ages of the Vedde and Saksunarvatn ashes and the Younger Dryas boundaries from Kråkenes, western Norway. *Journal of Quaternary Science* **29**: 506–507.

Long AJ, Roberts DH, Wright MR. 1999. Isolation basin stratigraphy and Holocene relative sea-level change on Arveprinsen Ejland, Disko Bugt, West Greenland. *Journal of Quaternary Science* **14**: 323–345.

Long AJ, Woodroffe SA, Roberts DH et al. 2011. Isolation basins, sea-level changes and the Holocene history of the Greenland Ice Sheet. *Quaternary Science Reviews* **30**: 3748–3768.

Newton AJ. 1996. Tephrabase: a tephrochronological database. *Quaternary Newsletter* **78**: 8–13.

Newton AJ, Dugmore AJ, Gittings BM. 2007. Tephrabase: tephrochronology and the development of a centralised European database. *Journal of Quaternary Science* **22**: 737–743.

Norðdahl H, Ásbjörnsdóttir L. 1995. Isaldarlok i Hvammsfirdi. In *Eyjar i Eldhafi*, Hroarsson B, Jónsson D, Jónsson SS (eds). Got mal: Reykjavik; 117–131.

Norðdahl H, Ingólfsson Ó, Pétursson HG et al. 2008. Late Weichselian and Holocene environmental history of Iceland. *Jökull* **58**: 343–364.

Norðdahl H, Pétursson HG. 2005. Relative sea-level changes in Iceland: new aspects of the Weichselian deglaciation of Iceland. In *Iceland: Modern Processes and Past Environments*, Caseldine C, Russell A, Harðardóttir J, Knudsen O (eds). Amsterdam: Elsevier 25–78.

Ólafsdóttir Þ. 1975. Jökulgarður á sjávarbotni út af Breiðafirði (English summary: A moraine ridge on the Iceland shelf, west of Breiðafjördur). *Náttúrufræðingurinn* **45**: 247–271.

Palmer AJM, Abbott WH. 1986. Diatoms as indicators of sea-level change. In *Sea-Level Research: a Manual for the Collection and Evaluation of Data*, Van Der Plassche O (ed.). Geo Books: Norwich. 457–487.

Persson C. 1971. Tephrochronological investigations of peat deposits in Scandinavia and on the Faroe Islands. *Sveriges Geologiska Undersökning Årbok* **65**: 1–34.

Principato SM. 2008. Geomorphic evidence for Holocene glacial advances and sea level fluctuations on eastern Vestfirðir, northwest Iceland. *Boreas* **37**: 132–145.

Reimer PJ, Bard E, Bayliss A et al. 2013. IntCal13 and Marine13 radiocarbon age calibration curves 0-50,000 years cal BP. *Radiocarbon* **55**: 1869–1887.

Rundgren M, Ingólfsson Ó. 1999. Plant survival in Iceland during periods of glaciation? *Journal of Biogeography* **26**: 387–396.

Rundgren M, Ingólfsson Ó, Björck S et al. 1997. Dynamic sea-level change during the last deglaciation of northern Iceland. *Boreas* **26**: 201–215.

Shennan I, Innes JB, Long AJ et al. 1994. Late Devensian and Holocene relative sealevel changes at Loch nan Eala, near Arisaig, northwest Scotland. *Journal of Quaternary Science* **9**: 261–283.

Shennan I, Lambeck K, Horton B et al. 2000. Late Devensian and Holocene records of relative sea-level changes in northwest Scotland and their implications for glacio-hydro-isostatic modelling. *Quaternary Science Reviews* **19**: 1103–1135.

Shennan I, Tooley M, Green F et al. 1999. Sea level, climate change and coastal evolution in Morar, northwest Scotland. *Geologie en Mijnbouw* **77**: 247–262.

Sigurdsson H. 1970. Structural origin and plate tectonics of the Snæfellsnes volcanic zone, Western Iceland. *Earth and Planetary Science Letters* **10**: 129–135.

Símonarson LA, Leifsdóttir ÓE. 2002. Late-Holocene sea-level changes in south and southwest Iceland reconstructed from littoral molluscan stratigraphy. *Holocene* **12**: 149–158.

Spagnolo M, Clark CD. 2009. A geomorphological overview of glacial landforms on the Icelandic continental shelf. *Journal of Maps* **5**: 37–52.

Stuiver M, Reimer PJ, Reimer RW. 2005. Calib 6.0 www program and associated documentation. calib.qub.ac.uk/calib/.

Tephrabase. 2012. Tephrabase: a tephrochronological database [Online]. Available: www.tephrabase.org [Accessed 3 June 2014].

Thors K, Helgadóttir G. 1991. Evidence from south west Iceland of low sea level in early Flandrian times. In *Environmental Change in Iceland: Past and Present*, Maizels JK, Caseldine C (eds). Kluwer: Dordrecht 93–104.

Troëls-Smith J. 1955. Characterisation of unconsolidated sediments. *Danmarks Geologiske Undersøgelse: Copenhagen* **3**: 1–73.

Van Der Plassche O. 1986. *Sea-level research: a manual for the collection and evaluation of data*. Geobooks: Norwich.